

# Fabrication and Characterization of Glassy Carbon MEMS

Olivier J. A. Schueller, Scott T. Brittain, Christian Marzolin, and G. M. Whitesides\*

Harvard University, Department of Chemistry and Chemical Biology, 12 Oxford Street, Cambridge, Massachusetts 02138

Received December 17, 1996<sup>®</sup>

This paper describes the fabrication of free-standing high-carbon microstructures by soft-lithographic techniques; these structures ranged in complexity from simple beams to complex, suspended deflectors. Microstructures of polymeric precursors (copolymers of furfuryl alcohol–phenol) to high-carbon solids were fabricated using poly(dimethylsiloxane) (PDMS) molds. Carbonization of these microstructures under argon resulted in mass loss (up to 45%) and shrinkage (up to 20% linearly); the density increased to reach a plateau value of  $\sim 1.5 \text{ g/cm}^3$  at  $\sim 900 \text{ }^\circ\text{C}$ . Microstructures pyrolyzed at  $900 \text{ }^\circ\text{C}$  were electrically conductive, with a conductivity of  $\sim 10^{-2} \Omega \text{ cm}$ . Elementary microelectromechanical functions were demonstrated in these microstructures: electrostatic actuation induced deflection or vibrations of suspended structures. The measurement of the frequency of resonance of high-carbon cantilevered beams allowed the determination of Young's modulus for the solid: typical values were  $\sim 15\text{--}20 \text{ GPa}$ . The microelectromechanical properties of more complex structures (microresonators, light deflectors) were also determined. This paper demonstrates that high-carbon microstructures can be easily fabricated that have potential use as the active components of MEMS.

## Introduction

This paper describes the preparation and characterization of carbon microelectromechanical systems (MEMS) fabricated by procedures based on micromolding of a polymeric precursor to form the carbon structure,<sup>1–3</sup> followed by thermal treatment to give it the desired electrical and mechanical properties.<sup>4,5</sup> This procedure is very different from that used in silicon micromachining, and the combination of material and process has the potential to generate many different types of devices.<sup>6–9</sup>

We have previously developed a wide array of techniques for the fabrication of microscopic and nanoscopic structures in organic polymers: these techniques include microcontact printing ( $\mu\text{CP}$ ) on planar and curved substrates,<sup>10,11</sup> micromolding in capillaries (MIMIC),<sup>1,12,13</sup>

and microtransfer molding ( $\mu\text{TM}$ ).<sup>3</sup> We have also demonstrated methods for rapid prototyping of these structures.<sup>14</sup> Here we describe the application of this set of techniques to the preparation of microstructures of polymers that are precursors to high-carbon solids, and the successful conversion of these polymers to functional high-carbon solids at high temperatures ( $400\text{--}1800 \text{ }^\circ\text{C}$ ) under an inert atmosphere. The resulting microstructures can be either free-standing or supported.<sup>15</sup> The overall shape of the microstructures is retained during carbonization, but the physical, mechanical, and chemical properties of these solids are strongly and controllably influenced by the heat treatment.

We are especially interested in the fabrication of microstructures of glassy carbon. Glassy (or vitreous) carbon is typically a hard solid prepared by heat-treatment at elevated temperatures ( $1000\text{--}3000 \text{ }^\circ\text{C}$ ) of polymeric precursors such as copolymer resins of phenol–formaldehyde or furfuryl alcohol–phenol.<sup>4,16</sup> These polymers are used because of their high carbon yield on pyrolysis (the ratio of carbon present after/before carbonization is  $\sim 50\%$ ).<sup>4</sup> The physical properties of glassy carbon make it a potential candidate for the preparation of MEMS. It is isotropic, electrically conducting, and impermeable to gases and has a low coefficient of thermal expansion. Glassy carbon has a lower density ( $1.3\text{--}1.5 \text{ g/cm}^3$ ) than graphite ( $2.27 \text{ g/cm}^3$ ) or diamond ( $3.52 \text{ g/cm}^3$ ); this density reflects its porous microstructure.<sup>16</sup> The voids constituting the pores are, however, not connected; this fact accounts for the low

<sup>®</sup> Abstract published in *Advance ACS Abstracts*, May 1, 1997.

- (1) Kim, E.; Xia, Y.; Whitesides, G. M. *Nature* **1995**, *376*, 581.
- (2) Xia, Y.; Kim, E.; Zhao, X.-M.; Rogers, J. A.; Prentiss, M.; Whitesides, G. M. *Science* **1996**, *273*, 344.
- (3) Zhao, X.-M.; Xia, Y.; Whitesides, G. M. *Adv. Mater.* **1996**, *8*, 420.
- (4) Jenkins, G. M.; Kawamura, K. *Polymeric Carbons—Carbon Fibre, Glass and Char*; Cambridge University Press: Cambridge, 1976.
- (5) Spain, I. L. In *Chemistry and Physics of Carbon*; Walker Jr., P. L.; Thrower, P. A., Eds.; Marcel Dekker, Inc.: New York, 1981; Vol. 16, p 119.
- (6) Delapierre, G. *Sensors Actuators* **1989**, *17*, 123.
- (7) Kovacs, G. T. A.; Petersen, K.; Albin, M. *Anal. Chem.* **1996**, *407A*.
- (8) Newell, W. E. *Science* **1968**, *161*, 1320.
- (9) Petersen, K. E. *IEEE Trans. Electron. Devices* **1978**, *ED-25*(10), 1241.
- (10) Jackman, R.; Wilbur, J. L.; Whitesides, G. M. *Science* **1995**, *269*, 664.
- (11) Wilbur, J. L.; Kumar, A.; Biebuyck, H. A.; Kim, E.; Whitesides, G. M. *Nanotechnology*, in press.
- (12) Kim, E.; Xia, Y.; Whitesides, G. M. *J. Am. Chem. Soc.* **1996**, *118*, 5722.
- (13) Xia, Y.; Kim, E.; Whitesides, G. M. *Chem. Mater.* **1996**, *8*, 1558.

(14) Qin, D.; Xia, Y.; Whitesides, G. M. *Adv. Mater.* **1996**, *8*, 917.

(15) Schueller, O. J. A.; Brittain, S. T.; Whitesides, G. M. *Adv. Mater.*, in press.

(16) Kinoshita, K. *Carbon, Electrochemical and Physicochemical Properties*; Wiley-Interscience: New York, 1988.

gas permeability observed for that material. Carbon is thermally stable in a non-oxidizing environment at temperatures higher than 3000 °C. Because of its high corrosion resistance and inertness under a wide variety of conditions, glassy carbon is used in extremely corrosive environments (for example, in crucibles for the decomposition of ores in analytical chemistry). Glassy carbon is also widely used as an electrode material for electrochemical applications.<sup>16–18</sup> It resists strong acids and bases and is inert over a wide range of electrical potentials.<sup>17</sup> The surface chemistry of glassy carbon allows tailoring of its interfacial properties (surface energy, electron-transfer kinetics) by physisorption or chemisorption of molecules, polymers, or metals, or by procedures involving electrochemical pretreatments, polishing, or laser activation.<sup>16–19</sup> Sensors and biosensors have been prepared by immobilization of recognition elements and enzymes on the surface of glassy carbon electrodes.<sup>16</sup>

Glassy carbon structures could be used in lieu of silicon in applications where lightweight, high chemical resistance to strong bases, or thermal stability are required properties. The lower Young's modulus of glassy carbon (10–40 GPa)<sup>4</sup> compared to that of silicon (190 GPa for monocrystalline silicon, 40–170 GPa for polysilicon)<sup>20</sup> can be an advantage in applications where the brittleness of silicon is a limiting factor, or where the extreme stiffness of silicon is a disadvantage (for example, in electrostatically driven actuators). Furthermore, silicon surfaces have a high surface energy since they are covered with a 10–20 Å thick native oxide layer. Surfaces with high free energies will be subjected to capillary forces when in close proximity. Stiction—that is, the adhesion between two surfaces—depends on van der Waals, electrostatic, and capillary forces.<sup>21</sup> The contribution of capillarity accounts for most of the forces responsible for stiction. Stiction often limits the performance of MEMS: once two surfaces are in contact, only a restoring force can separate them. The density of oxygen-containing, polar surface functional groups is lower on carbon (typically 2–10%) than on Si/SiO<sub>2</sub>. The ability to functionalize the surface of oxidized carbon further to introduce hydrocarbon or fluorocarbon groups offers a route to materials with very low surface free energies and low potential for stiction.<sup>16,21,22</sup> The relatively rough surface of carbon solids (relative to silicon etched along a crystal face) may also prevent stiction since the true area of contact between rough surfaces is smaller than between smoother surfaces.<sup>23</sup>

This paper is organized in two parts. In the first part, we describe the fabrication of structures and micro-

structures of various degrees of complexity. In the second part, we report initial testing of the microelectromechanical properties of these structures.

## Results and Discussion

**Fabrication of Microstructures.** MEMS are typically prepared from silicon or occasionally from other materials (gallium arsenide, metals, glasses, ceramics, or plastics) by microfabrication techniques that have been exhaustively developed in the integrated circuit industry.<sup>7</sup> These techniques rely heavily on photolithography and selective etching procedures and therefore require the design of chrome masks, access to a clean room, and use of other facilities used in microfabrication. We have relied on the less expensive soft-lithographic techniques that we have developed: a key element in these techniques is the availability of convenient, inexpensive methods for the preparation of polydimethylsiloxane (PDMS) molds that are used throughout these techniques, and the use of these PDMS molds to generate microstructures in polymeric materials that are precursors to carbon solids.

The PDMS molds were prepared as described previously, by casting PDMS on a photographically generated master.<sup>3,24,25</sup> The masks used in photolithography were generated by rapid prototyping.<sup>14,26</sup> In this technique, a computer file of the design of interest was generated using Freehand 5.5. The file was printed on a transparent film with a high-resolution (>3300 dpi) printer, and that transparent film was used as a mask to generate surface relief patterns in films of photoresists coated on Si wafers. This technique has a very short turnaround time and therefore allows many structures to be prepared and tested.<sup>14</sup> Changes in the design of microstructures can be readily implemented in order to compensate for unexpected flaws in a structure. Numerous low-cost iterations can be performed using rapid prototyping.

The carbon precursor used in the present study was a furfuryl alcohol-modified phenolic resin. This type of polymer is widely used as a precursor to carbon solids because of its low cost and relatively high carbon yield (~50%).<sup>4,27</sup> Patterns of that polymer were generated by either MIMIC or  $\mu$ TM. In MIMIC, the liquid polymer spontaneously fills the capillary channels defined by a surface relief of the PDMS mold in conformal contact with a substrate.<sup>1,12,13</sup> This technique is ideal for the preparation of continuous structures such as wires and grids (Figure 1). On the other hand,  $\mu$ TM allows the formation of discrete, unconnected structures (Figure 2).<sup>3</sup> In  $\mu$ TM, the liquid polymer is applied to the recessed patterns of the PDMS mold. The excess polymer is removed by gently scraping with the edge of a second piece of PDMS. The PDMS mold is placed in contact with the substrate; this contact constrains the remaining polymer in the recessed channels of the mold. We observed that an excessive quantity of polymer prevents conformal contact of the PDMS mold with the

(17) van der Linden, W. E.; Dieker, J. W. *Anal. Chim. Acta* **1980**, *119*, 1.

(18) McCreery, R. L. In *Bard, A. J. Ed.; Marcel Dekker: New York, 1991; Vol. 17, p 221.*

(19) Pocard, N. L.; Alsmeyer, D. C.; McCreery, R. L.; Neenan, T. X.; Callstrom, M. R. *J. Mater. Chem.* **1992**, *2*, 771.

(20) Guo, S.; Zou, D.; Wang, W. In *Smart Materials Fabrication and Materials for Micro-Electro-Mechanical Systems*; San Francisco, CA, 1992; Materials Research Society Symposium Proceedings, Vol. 276, p 233.

(21) Houston, M. R.; Howe, R. T.; Komvopoulos, K.; Maboudian, R. In *Mechanical Behavior of Diamond and Other Forms of Carbon. Symposium*; San Francisco, CA, 1995; Vol. 383, p 391.

(22) Hoekstra, K. J.; Bein, T. *Chem. Mater.* **1996**, *8*, 1865.

(23) Houston, M. R.; Maboudian, R.; Howe, R. T. In *Proceedings of the 8th International Conference on Solid-State Sensors and Actuators Conference—TRANSDUCERS'95*; Stockholm, Sweden, 1995; Vol. 1, p 210.

(24) Kumar, A.; Whitesides, G. M. *Appl. Phys. Lett.* **1993**, *63*, 2002.

(25) Kumar, A.; Biebuyck, H. A.; Whitesides, G. M. *Langmuir* **1994**, *10*, 1498.

(26) Economical mask-making procedures using desktop publishing is also described at <http://mems.isi.edu/archives/tools/PSMASKMAKER/> by Ash Parameswaran, Simon Fraser University, Burnaby, BC, Canada.

(27) Fitzer, E.; Mueller, K.; Schaefer, W. In *Chemistry and Physics of Carbon*; Walker Jr., P. L., Ed.; Marcel Dekker: New York, 1971; Vol. 7, p 237.

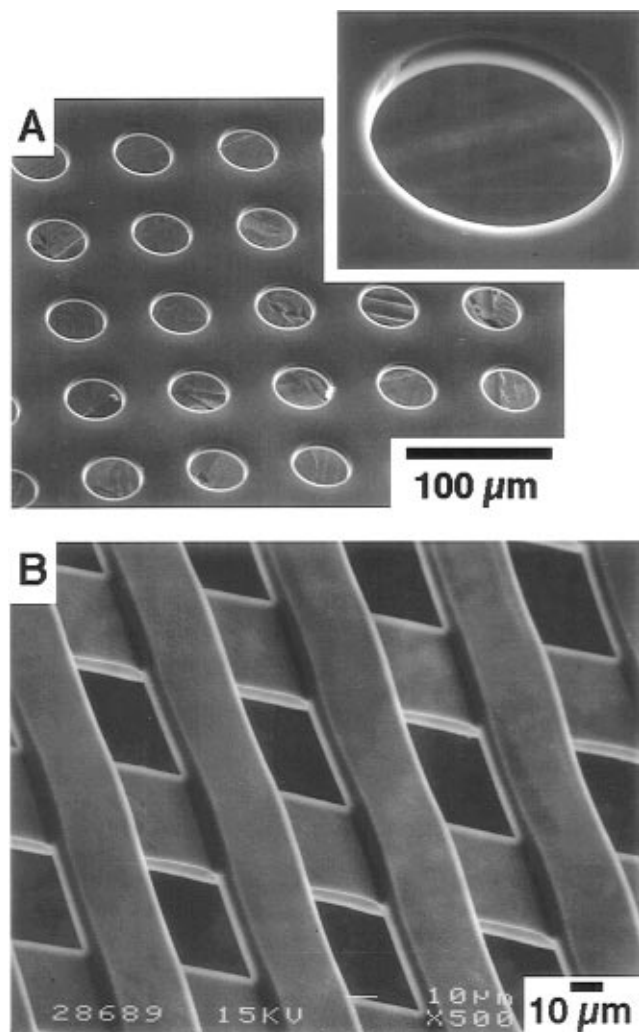


**Figure 1.** Scanning electron micrographs of conductive carbon grids prepared by carbonization at 800 °C of a furfuryl alcohol-based resin patterned by MIMIC. The liquid polymer filled the channels defined by the PDMS mold in conformal contact with a substrate, and was cured. The polymeric grid was then lifted off the substrate and sandwiched between silicon wafers during carbonization to prevent buckling. (A) This conductive grid was prepared with a PDMS mold consisting of 50  $\mu\text{m}$  pillars spaced by 50  $\mu\text{m}$ . When placing this mold face down on a substrate, only the pillars are in contact with the substrate. The thickness of the film is determined by the depth of the surface relief of the mold and shrinkage during carbonization. The surface of the conductive carbon tape used for mounting the sample is visible through the holes of the film. (B) The bilayered grid was prepared by MIMIC between two PDMS stamps with their patterns (50  $\mu\text{m}$  lines spaced by 50  $\mu\text{m}$ ) perpendicular to each other.

substrate. In this case, a thick film of polymer formed between the PDMS mold and the substrate that induced dewetting of the recessed structures. It was therefore important to minimize the quantity of polymer applied to the stamp. The liquid polymer was cured within the mold by placing the substrate on a hot plate. The surface temperature was increased slowly from  $\sim 80$  to 150 °C over  $\sim 45$ –60 min in order to induce further cross-linking of the liquid polymers. A fast cure distorted or destroyed the structure. Prolonged contact between the PDMS mold and the polymer was also detrimental, as the cured polymer tended to remain trapped in the mold rather than being transferred to the substrate. We obtained reproducible results when the procedure (application of the polymer followed by

curing) was performed in less than 1.5 h.

After completion of the curing step, the PDMS mold was removed, and the supported polymeric structures were converted into free-standing high-carbon structures by carbonization (400–1000 °C) under an inert atmosphere (argon). In some cases, we observed (after completion of the curing step) the presence of a very thin film ( $\sim 100$  nm) connecting the discrete structures dispersed on the surface. The thickness of the film was small compared to that of the microstructures; in general, it did not survive the thermal processing and the mechanical stress introduced during carbonization. If it did survive, it was easily removed after the carbonization step by gently blowing on the microstructures.

The substrates used in the present study consisted of silicon wafers coated with thin chromium films (400 Å) prepared by electron beam evaporation. We found that, unlike other substrates, the chromium on silicon substrates prevented fracture of the structures during carbonization. The structures spontaneously released from the chromium surface as they shrank. Substrates that were unsuccessfully tested include silica, silicon wafers, commercially available glassy carbon pellets, and titanium, nickel, silver, or gold films on silicon/SiO<sub>2</sub> wafers. It is unclear why chromium performed better than other metals, but we hypothesize that its high melting point (1857 °C) and lower chemical reactivity may be important factors.

In the work reported here, the lateral dimensions of the microstructures are determined by the resolution of the rapid prototyping technique:<sup>14</sup> we have found that this technique is quite practical for the preparation of structures with features  $> 20$   $\mu\text{m}$ ; for smaller features, we believe that other techniques will be successful, but we have not yet explored these smaller structures. The PDMS molds prepared on these patterns reproduce with fidelity the edge roughness ( $\sim 1$   $\mu\text{m}$ ) of the original photolithographic master, and this low edge resolution is transferred to the polymers used in  $\mu\text{TM}$ . The thickness of the microstructures is determined by the depth of the surface relief in the PDMS mold, i.e., the thickness of the film of photoresist used to produce the master. Thicker patterns of photoresist were prepared by spin-coating successive films of photoresist and soft-baking each film after application to the wafer. We were able to obtain thick patterns of photoresist (up to 40  $\mu\text{m}$ ) by spin-coating four films of photoresist prior to exposure.

**Characterization of the Carbon Solids.** The evolution of the density, the weight loss, and the lateral shrinkage experienced by the solids as a function of heat-treatment temperature were investigated and are plotted in Figure 3. The density of the cured polymer before carbonization was 1.29 g/cm<sup>3</sup>. The density (measured at room temperature) reached a minimum of 1.22 g/cm<sup>3</sup> at 400 °C before increasing to 1.51 g/cm<sup>3</sup> at 1000 °C. The trend and values are in good agreement with literature reports.<sup>4,27</sup> The weight loss is attributed to the elimination of solvent and unreacted monomers and to the elimination of heteroatoms. A total weight loss of  $\sim 45\%$  occurs by  $\sim 800$  °C. Shrinkage of the solid appears to be isotropic and steady over the range of temperatures investigated. At 800 °C, the solid has shrunk by  $\sim 20\%$ . Above that temperature, additional

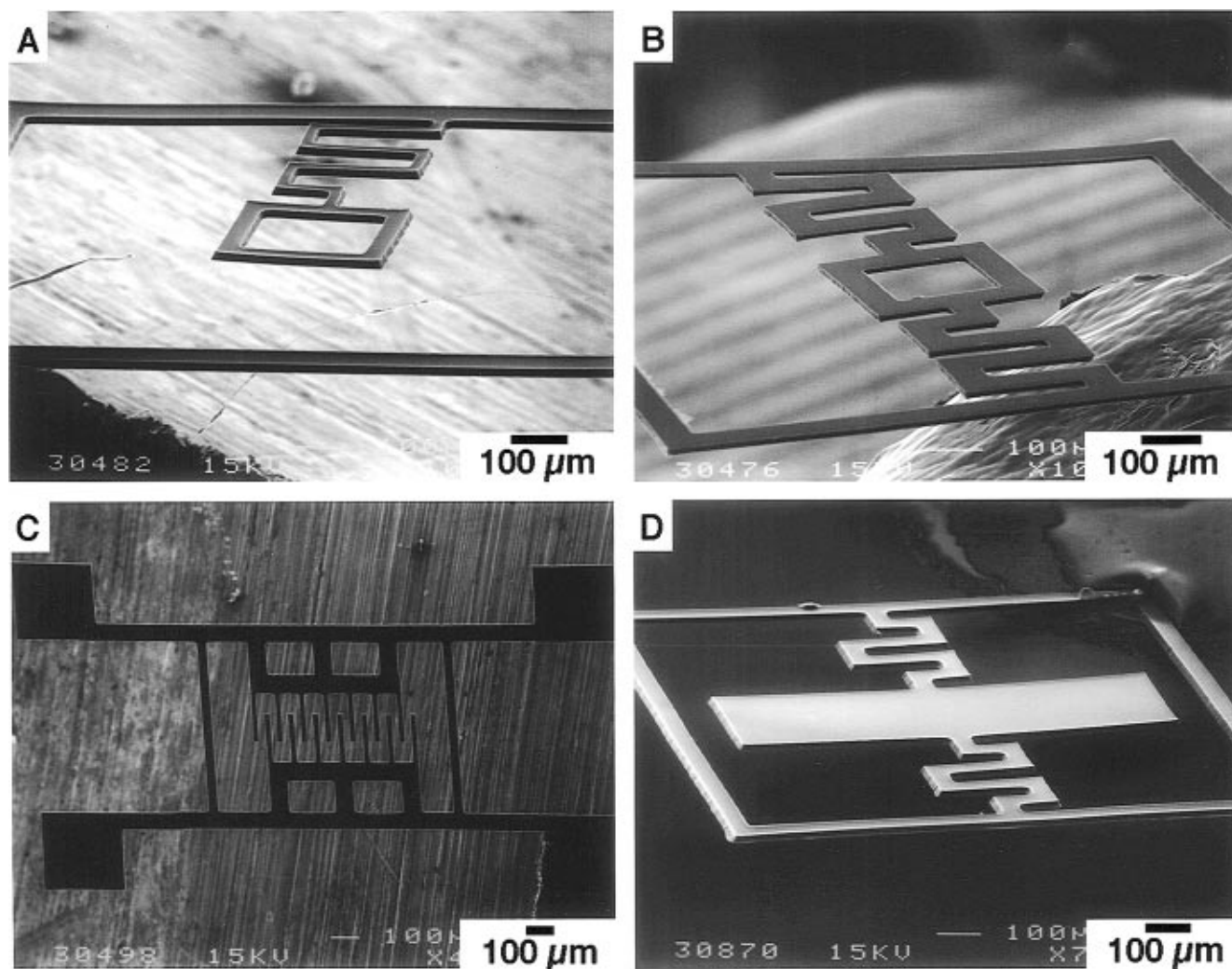


**Figure 2.** Scanning electron micrographs of carbon structures prepared by carbonization at 1000 °C of a resin patterned by  $\mu$ TM. (A) and (B) The inner frame can be electrostatically actuated. This type of structure represents the sensing unit for an accelerometer. (C) Precursor to an interdigitated capacitor. The interdigitated comb structures become electrically isolated once the supporting frame is broken. (D) Optical deflector. The initial carbonization step at 1000 °C (in a tube furnace) was followed by heat treatment under Ar up to 1800 °C (in an induction furnace). Electrostatic actuation can induce angular deflection of the central plate. The angle of deflection of a light beam reflected off the surface of the central plate can therefore be controlled electrostatically.

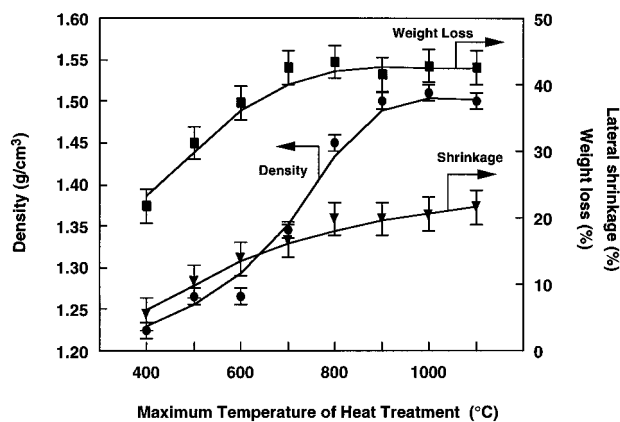


**Figure 3.** Evolution of the density, weight loss, and shrinkage of a furfuryl alcohol-based resin as a function of temperature of heat treatment. The density was determined by flotation. The dimensions and weight of the solids were measured before and after carbonization.

shrinkage is minimal (<3%). By anticipating a linear shrinkage of 20%, the lateral dimensions as well as the thickness of the carbon microstructures can be predicted

well from the dimensions of the initial photoresist pattern.

**Evolution of the Microstructures during Carbonization: Differentiation between Surfaces.** Figure 4A shows scanning electron micrographs of the surface of the carbon solid in contact with the chromium substrate (bottom) and on the surface away from the chromium substrate (top) during curing and carbonization. The bottom surface remained featureless during carbonization and appeared smooth by electron microscopy, whereas the top surface was slightly curved and dimpled. The dimples (0.5–1  $\mu$ m wide, 0.1–0.2  $\mu$ m deep) are probably due to the outgassing of the solvent during polymerization. The presence of these dimples will affect the reflective properties of the carbon surface as light will be scattered by the irregularities of the surface. The surface composition of the carbon solids prepared by heat treatment at 1000 °C was investigated by X-ray photoelectron spectroscopy (XPS). Figure 4B shows XPS survey spectra performed on the top and the bottom surfaces. The atomic compositions of both surfaces are similar, consisting mainly of carbon (>90%) and oxygen (up to 8%). Chromium and zinc (<1% each)

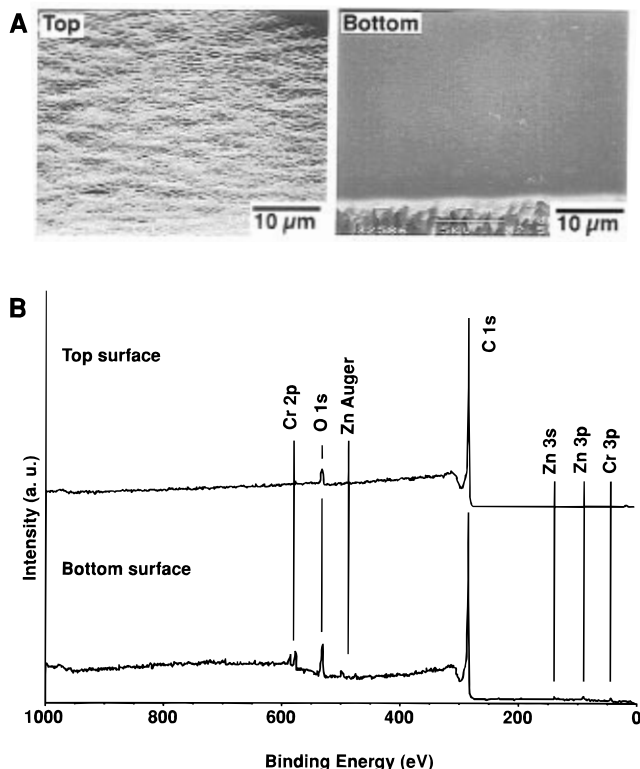


**Figure 4.** (A) Scanning electron micrographs of the top and bottom surfaces of a carbon solid prepared by curing and carbonization at 1000 °C under argon of a furfuryl alcohol-based resin on a chromium thin film (400 Å) on Si. The dimples observed on the top surface are attributed to outgassing during heat treatment. The bottom surface, which was in contact with the chromium substrate throughout the carbonization process, remained featureless. The lower portion of the micrograph displays the edge of the microstructure, imaged to ensure proper focus. (B) XPS survey spectra of the top and bottom surfaces of the high-carbon solid shown in (A).

are detected on the bottom surface but not on the top surface. The presence of zinc stems from the fact that a solution of  $\text{ZnCl}_2$  was introduced into the resin in order to catalyze its polymerization to a cross-linked solid. The oxygen concentration is twice as high on the bottom surface (8%), suggesting that the residual metals may be present as metal oxides.

Shrinking during carbonization reduces the dimensions of the microstructures. It is also responsible for the slight buckling consistently observed on carbonaceous microstructures. Once the PDMS mold filled with the liquid resin, whether by MIMIC or  $\mu\text{TM}$ , the temperature was increased in order to induce curing. The viscosity of the polymer decreased as the temperature increased; this decrease in viscosity, coupled with the increase in density as the polymerization proceeded, resulted in sagging of the polymeric liquid within the capillary channels. The large coefficient of thermal expansion of PDMS ( $\sim 10^{-5}$  m/(K m)) may also have contributed to the deformation of the mold during curing. When the temperature of curing was reached, the sagged polymeric structure solidified. While the bottom of the microstructure (the part in direct contact with the planar substrate) remained flat, the top of the microstructure became slightly curved during curing. Further carbonization and densification accentuated the buckling of the microstructure.

**Microelectromechanical Functions.** We investigated the microelectromechanical functions of these

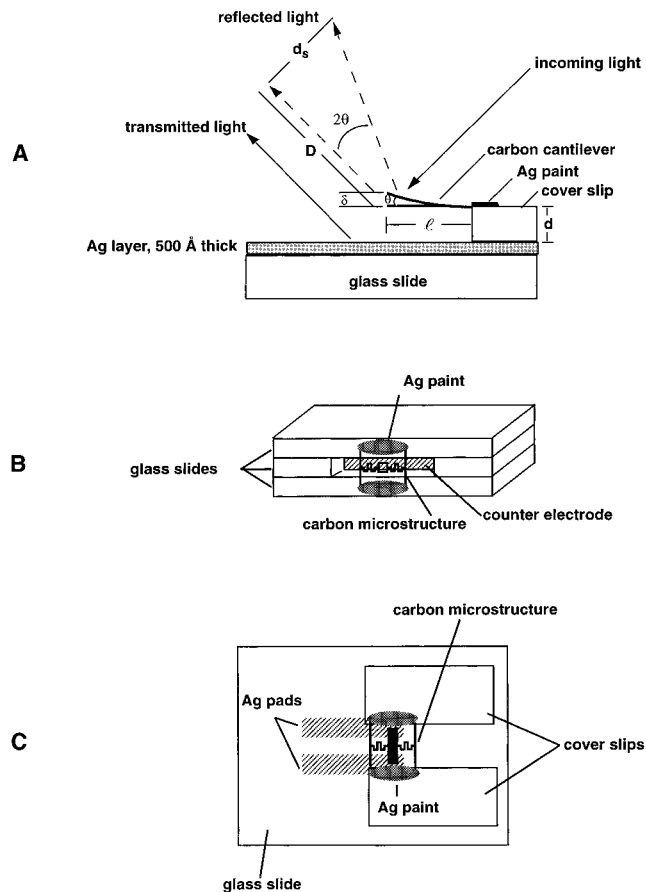


**Figure 5.** (A) Experimental setup for the testing of the mechanical properties of a cantilever beam. A cantilever beam was glued with conductive silver paint to a cover slip (150  $\mu\text{m}$  thick) so that it was suspended over the edge of the slip for most of its length. The cover slip was then affixed to a glass slide coated with a thin film of silver (500 Å), with the carbon beam overhanging the silver thin film. An ac voltage was applied between the thin film and the cantilever beam in order to drive the beam to resonance. The motion of the beam was detected optically. A laser light was focused on the extremity of the beam, and the modulation in either reflected (off the beam) or transmitted (reflected off the silver thin film) light was detected and recorded with an oscilloscope. By measuring the displacement  $d_s$  of a projected spot on a screen located at a known distance  $D$  from the beam, we were able to calculate the angular displacement  $\theta$  as well as the linear displacement  $\delta$  of the extremity of the beam. (B) Experimental setup for measuring the frequency of uniaxial vibrations of a carbon microstructure. A carbon microstructure glued between the top and the bottom glass slides could be electrostatically actuated by applying a voltage between the microstructure and the counterelectrode. The counterelectrode can slide independently between the top and the bottom glass slides. The distance between the microstructure and the counterelectrode could be adjusted with a micropositioning translational stage. (C) Experimental setup for measuring the deflection of a microstructure. The distance between the MEMS and the silver counterelectrodes is preset by the thickness of the cover slip. The silver counterelectrodes can be addressed independently. Deflection is induced by a combination of attractive and repulsive forces.

high-carbon structures. As the microstructures are free-standing, they were mounted by hand (Figure 5). The structures were typically glued with conductive silver paint on an insulating substrate (glass slides, polyimide films). The resistivity of the carbon solids prepared at 1000 °C is  $\sim 0.03$   $\Omega$  cm. Application of a voltage between the carbonaceous microstructure and a counterelectrode

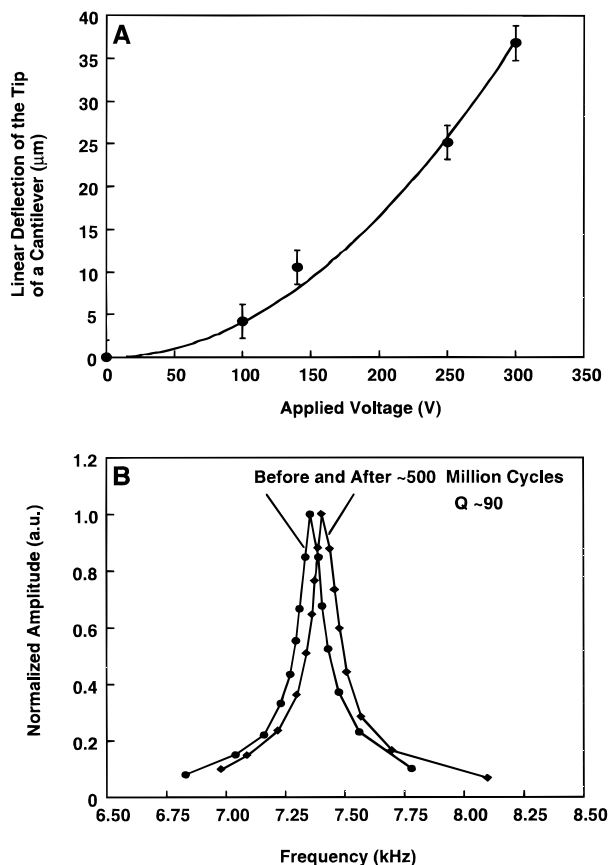


**Figure 6.** (A) Linear deflection of the tip of a 1.17-mm long, 6- $\mu\text{m}$  thick cantilevered beam prepared by carbonization (1000  $^{\circ}\text{C}$ ) of a furfuryl alcohol-modified phenolic resin assembled by MIMIC as a function of applied dc voltage. The deflection was calculated from the displacement of a spot reflected off the top of the cantilever on a screen located 28 cm away. The projected spot moved up to 18 mm. (B) Resonance frequency of a 1.14-mm long, 17- $\mu\text{m}$  thick cantilevered beam prepared by carbonization (1000  $^{\circ}\text{C}$ ) of a furfuryl alcohol-modified phenolic resin assembled by  $\mu\text{TM}$ . The frequency of resonance ( $\sim 7.4$  kHz) and the quality factor ( $Q \sim 90$ ) remained unchanged within the error of measurements (0.05 kHz) after vibration at resonance for 22 h ( $> 500$  million cycles).

in close proximity generated an electrostatic force between both electrodes and induced a deflection. A photodiode recorded the modulation of the laser beam by the moving part.

(a) *Cantilevered Beams.* We tested simple structures such as suspended beams fixed at one end (Figure 5A). Individual carbon beams obtained by clipping comb structures prepared by MIMIC were used for the sake of simplicity, but arrays of suspended beams could have been tested as easily; these arrays would give access to a large range of vibrations determined by the length of each beam.<sup>28</sup> We were able to measure the frequency of vibrations of beams in both reflection and transmission modes. In both cases, the laser beam was focused on the end of the beam. In reflection mode, we recorded the displacement of a reflected light spot projected on a screen. The reflection mode was used for the determination of the deflection of the end of the beam. In transmission mode, we recorded the modulation of the

light reflected by the surface of the silver counterelectrode. The transmission mode was more useful for the determination of the natural frequencies of vibrations.

The deflection of the tip of a cantilever beam (1.17 mm long) as a function of applied dc voltage is plotted in Figure 6A. The deflection of the tip of the cantilever was calculated with eqs 1 and 2 based on simple geometric considerations:

$$\delta = l \sin \theta \quad (1)$$

$$d_s = D \tan 2\theta \quad (2)$$

where  $\delta$  represents the deflection of the tip of the cantilever,  $l$  the length of the cantilever,  $\theta$  the angular displacement of the cantilever, and  $d_s$  the displacement of the projected spot on a screen located at a distance  $D$  from the cantilever.

The voltage required to induce deflection of the beam is large but would be much smaller if the distance between the MEMS and the counterelectrode were smaller. The deflection of the tip can be fitted to a second-order polynomial, indicating that the electrostatic force can be approximated to a localized force applied vertically at the extremity of the beam.

Young's modulus of the carbon solid can be deduced from the resonance frequencies  $f_r$  of vibrations of a cantilever beam using eq 3:<sup>29</sup>

$$f_r = \frac{1}{2\pi} \left( \frac{EI\lambda_r^4}{A\rho l^3} \right)^{1/2} \quad (3)$$

where  $f_r$  is the frequency of resonance,  $E$  is Young's modulus,  $I$  is the moment of inertia of the cantilever beam,  $l$  is the length of the beam,  $A$  is the cross section of the cantilever perpendicular to the length,  $\rho$  is the density of the material, and  $\lambda_r$  is the root of the frequency equation (4). For a beam of rectangular cross-section (width  $w$ , thickness  $t$ ),  $I = wt^3/12$ .

$$1 + \cos \lambda \cosh \lambda = 0 \quad (4)$$

This equation has an infinite number of real positive roots. The first three roots are  $\lambda_1 \sim 1.87510$ ,  $\lambda_2 \sim 4.69409$ , and  $\lambda_3 \sim 7.85476$ . Each of these roots corresponds to a resonance frequency  $f_r$  that satisfies eq 3.<sup>29</sup>

The resonance frequencies can be determined by two different methods. In the forced oscillations mode, an ac voltage is applied between the microstructure and the counterelectrode. The frequencies ( $f_1, f_2, \dots$ ) at which the cantilever beam is in resonance with the applied voltage are recorded. In the free oscillations mode, the cantilever is excited with a short pulse and relaxes at its resonance frequency of vibration ( $f_i$ ). Both approaches allow the determination of the quality factor  $Q$ , which characterizes dissipation. The quality factor is defined by eq 5,

$$Q = \frac{f_r}{|\nu_1 - \nu_2|} \quad (5)$$

where  $\nu_1$  and  $\nu_2$  are the frequencies of vibration off-resonance at which the amplitude of the signal is equal to the maximum signal amplitude (i.e., at resonance) divided by  $\sqrt{2}$ .<sup>29</sup>

(28) Haronian, D.; MacDonald, N. C. *Sensors Actuators* **1996**, *A53*, 288.

(29) Sneddon, I. N. *Encyclopaedic Dictionary of Mathematics for Engineers and Applied Scientists*; Pergamon Press: New York, 1976.

**Table 1. Determination of Young's Modulus for Carbon Cantilevered Beams Prepared by Carbonization at 1000 °C**

length ( $\mu\text{m}$ )	thickness ( $\mu\text{m}$ )	density ( $\text{g}/\text{cm}^3$ )	frequency <sup>a</sup> (kHz)	Young's modulus (GPa)
1130	6	1.51	2.55	18
			15.8	17
1170	6	1.51	2.20	15
			14.3	16
1400	6	1.51	1.58	16
			10.0	16
1140	17	1.51	7.35	18
			43.5	14

<sup>a</sup> Young's modulus can be determined from either the 1st or 2nd resonant frequencies of the carbon cantilevers.

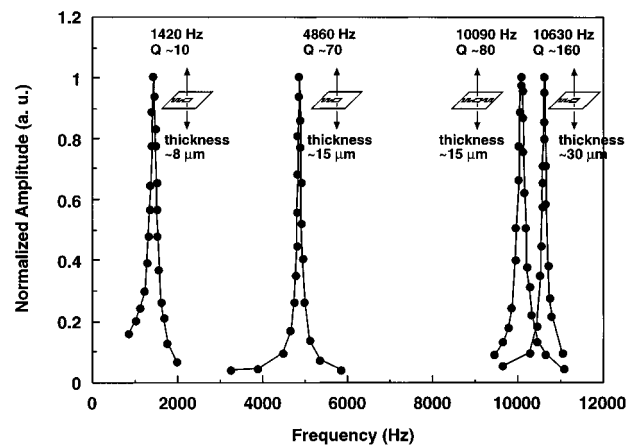
We measured the resonant frequencies of vibration of cantilevered beams of different lengths and thicknesses and deduced Young's modulus for carbon solids prepared by heat treatment at 1000 °C (Table 1). The value of Young's modulus ( $\sim 15$ – $20$  GPa) is consistent with values reported for carbon solids prepared under similar conditions.<sup>4</sup> Low-quality factors (10–20) were measured for thin (6  $\mu\text{m}$ ) vibrating beams operated at ambient pressure in air. Higher quality factors ( $\sim 90$ ) were obtained for thicker beams (17  $\mu\text{m}$ ). Air damping is the dominant mechanism for the dissipation of energy. Much higher quality factors would be measured if the experiment were performed under reduced pressure.<sup>8,30–33</sup>

Figure 6B plots the variation of the amplitude of vibration for a thicker ( $\sim 17$   $\mu\text{m}$ ) carbon cantilevered beam as a function of the frequency of the applied ac voltage. The small difference ( $\sim 50$  Hz, less than 1%) in the frequency of resonance ( $\sim 7.4$  kHz) after continuous operation for  $>500$  million cycles is within the margin of error for our measurements.

(b) *Complex Microstructures.* We tested the microelectromechanical properties of microstructures such as those displayed in Figure 2. These structures were mounted as depicted in Figure 5B,C, respectively. The determination of Young's modulus from the frequencies of vibration of these microstructures is complicated by their more complex geometries and is beyond the scope of this paper.

Capacitive sensors generate an electrical signal as a result of the displacement of a suspended electrode relative to a fixed electrode.<sup>34</sup> As the distance between the electrodes constituting the capacitor changes, so does the capacitance of the capacitor defined by the geometry of the system. Numerous pressure-sensing devices and accelerometers have been prepared that rely on changes in capacitance.<sup>34</sup>

The carbon microstructure displayed in Figure 2B could potentially be used as an uniaxial accelerometer: the vertical displacement of the suspended inner frame induced by acceleration or deceleration would induce a change in the capacitance between the carbon microstructures and a counterelectrode. We prepared microstructures with one or two supporting arms extending



**Figure 7.** Amplitude of resonance of suspended microstructures with one or two supporting arms as a function of frequency of applied ac voltage. The thickness of the microstructures is either  $\sim 8$ ,  $\sim 15$ , or  $\sim 30$   $\mu\text{m}$ . The width of the carbon frame and of the beams is  $\sim 70$   $\mu\text{m}$ . The width of the path traced by the zigzag is  $\sim 250$   $\mu\text{m}$ . Both the frequency of resonance and the  $Q$ -factor increase with the thickness of the microstructures.

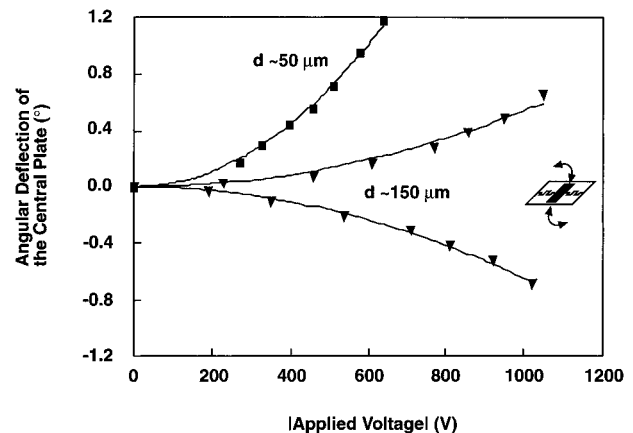


**Figure 8.** Angular deflection of the central plate of a display unit as a function of applied voltage. The distance between the carbon microstructure and the counterelectrode, determined by the thickness of the cover slips or insulating films used in the experimental setup, has a strong influence on deflection. Lower voltage is required to induce larger deflection when the distance between both electrodes is smaller.

from the outer frame to the inner frame. The zigzag design of the supporting arms greatly reduces the probability of fracture of the microstructures during carbonization, relative to microstructures with straight supporting beams. This difference is probably due to the fact that shrinkage is distributed over the entire zigzag rather than concentrated unidirectionally in a simple beam. Vibrations of the inner frame were electrostatically induced as indicated in Figure 5B. The modulation of a laser beam by the vibrating structure was recorded with a photodiode. Figure 7 plots the variation of the amplitude of vibration for carbon microstructures of different thickness as a function of the frequency of the applied ac voltage. Higher-order resonances were also recorded at higher frequencies (up to 85 kHz) for some of these structures.

The microstructure displayed in Figure 2D is the basic unit for a rudimentary display system when mounted as shown in Figure 5C. The microstructure is glued over the edges of two cover slips separated by  $\sim 1$  mm. The central plate is electrostatically actuated simulta-

(30) Buser, R. A.; De Rooij, N. F. *Sensors Actuators* **1989**, *17*, 145.

(31) Buser, R. A.; De Rooij, N. F. *Sensors Actuators* **1990**, *A21–A23*, 323.

(32) Mihailovich, R. E.; MacDonald, N. C. *Sensors Actuators* **1995**, *A50*, 199.

(33) Seidel, H.; Riedel, H.; Kolbeck, R.; Mück, G.; Kupke, W.; Königer, M. *Sensors Actuators* **1990**, *A21–A23*, 312.

(34) Puers, R. *Sensors Actuators* **1993**, *A37*, 93.

neously by attractive and repulsive forces: a voltage is applied between the carbon structure and one of the underlying silver electrodes (attractive), while the second silver electrode is held at the same potential as the carbon structure (repulsive). The angle of deflection of a light beam directed toward the structure can therefore be controlled electrostatically.

The angular deflection of the central plate as a function of applied voltage is plotted in Figure 8. The deflection depends on several factors including applied voltage, distance between the moving carbon element of the microstructure and the counter electrodes, and spring constant of the microstructure. The distance between the carbon microstructure and the counter electrodes is determined by the thickness of the insulating layer (glass cover slips or polyimide films) used in the procedure. As the thickness of that layer decreases, so does the voltage required to actuate the central plate. The structural dimensions and mechanical properties of the carbon solid define the spring constant of the structure. The mechanical properties of the material are, of course, primarily defined by the temperature of pyrolysis, but design will enable the deflection to be optimized by control of thickness, width, and dimensions of the supporting arms.

### Conclusions

High-carbon microstructures with complex geometries were fabricated by pyrolysis of organic polymers patterned by soft-lithographic techniques. The polymers were fabricated in PDMS molds. The entire procedure, from conception of a design, through production of the mold by rapid prototyping, to pyrolysis of the polymeric microstructures, can be performed in less than 24 h and requires only one photolithographic step. Polymers with high carbon yield (~50%) were used as precursors to high-carbon solids in order to minimize the detrimental effects of mass loss and shrinkage.

The inherent conductivity of the carbon solids prepared at 1000 °C enabled their use as part of the electrical circuitry required for their actuation. Vibrations and/or deflections of cantilevered beams or suspended structures were induced electrostatically. Young's modulus was calculated from the natural frequency of resonance of simple structures such as cantilevered beams. Young's modulus for high-carbon solids prepared by carbonization at 1000 °C is ~17 GPa. We are currently investigating the influence of the carbonization conditions on the evolution of the mechanical properties (Young's modulus) of the solids. The use of computer modeling will allow the optimization of the microelectromechanical properties of the microstructures.

The rapid prototyping technique combined with  $\mu$ TM is ideal for the preparation of polymeric microstructures (feature size  $\geq 20 \mu\text{m}$ ) that can be converted to high-carbon microstructures by carbonization. The ability to fabricate complex carbon microstructures combined with their electrical, mechanical, and chemical properties make them attractive candidates for use as com-

ponents in MEMS in conditions under which silicon would fail.

### Experimental Section

**Fabrication of the Microstructures.** Fabrication of the PDMS molds was performed according to procedures previously reported.<sup>24,25</sup> The PDMS molds were prepared by casting PDMS (Sylgard 184, Dow Corning) on photolithographically generated masters consisting of patterned films of photoresist (Microposit STR 1075, Shipley, MA). The masks used in the photolithographic step were prepared by rapid prototyping.<sup>14</sup> The substrates used for the preparation of the polymeric microstructures and subsequent carbonization were obtained by e-beam evaporation of chromium thin films (400 Å) onto silicon wafers. The furfuryl alcohol-modified phenolic resin was obtained from Q.O. Chemicals (Furcarb LP-520). Curing of the latter resin required the addition of a latent, heat-activated catalyst such as a 50% aqueous solution of  $\text{ZnCl}_2$ . The amount of catalyst never exceeded 10% (w/w) of the resin in order to prevent a too rapid cure and potential deformation of the microstructures. **Caution:** Mixing an acid catalyst with furfuryl alcohol-based resins induces an exothermic reaction. Curing of the polymer was usually performed on a calibrated hot plate. Carbonization was performed in a Blue M/Lindberg MiniMite tube furnace fitted with a quartz tube. The samples were placed in an alumina boat and introduced in the quartz tube. The chamber was deoxygenated by a rapid flow of argon for ~20 min prior to carbonization. Carbonization was performed under a positive pressure of argon. The temperature increased at a rate of 5 °C/min up to the final temperature. The samples were kept at the final temperature for 10 min and then let cool to room temperature.

**Characterization of the Carbon Solids.** Resistance measurements were performed with a hand-held voltmeter. The density of the solids was estimated by floating the solids in liquids of known densities. One limitation of this technique is that it underestimates densities of solids containing hydrophobic voids, which trap gas. Liquids used (density in  $\text{g/cm}^3$ ): nitrobenzene (1.197), 1,2-dichloroethane (1.256), 1-bromobutane (1.276), 1,1,1-trichloroethane (1.338), 1-bromopropane (1.354), trichloroacetonitrile (1.440), bromoethane (1.460), bromobenzene (1.491), 1,7-dibromoheptane (1.510). SEM was performed on a JEOL JSM-6400 scanning electron microscope operated at 15 keV. The samples were either glued to conductive carbon tape or glued to a silicon substrate with silver paint. X-ray photoelectron spectra were obtained on a SSX-100 spectrometer (Surface Science Laboratories) using a monochromatic Al  $K\alpha$  X-ray source. The spot size was ~1 mm<sup>2</sup> with an analyzer pass energy of 150 eV.

**Testing of the Microelectromechanical Properties.** The carbon microstructures were glued with silver paint onto glass slides (Figure 5). The counterelectrode in Figure 5A consisted of a silver thin film (500 Å) on glass prepared by e-beam evaporation. The counterelectrode in Figure 5B consisted of a metallized piece of a silicon wafer glued on the edge of a glass slide. The silver counterelectrodes used for the testing of the deflector (Figure 5C) were prepared by etching a silver thin film protected with self-assembled monolayers.<sup>35,36</sup> An ac or dc voltage was applied between the microstructure and the counterelectrode using a function generator (Wavetek Model 187 (San Diego, CA)) and an amplifier (Burleigh high-voltage DC OP AMP PZ-73). Frequencies of vibrations were measured by recording the modulation of a He-Ne laser (633 nm) by the moving structure using a photodiode and an oscilloscope (Tektronix 2445A).

**Acknowledgment.** This work was supported in part by the Office of Naval Research and the Defense Advanced Research Projects Agency. It used MRSEC Shared Facilities supported by the National Science Foundation (DMR-9400396). The authors thank Yuan Lu for his help with the XPS and Joe Tien for helpful discussion regarding photolithography.

(35) Xia, Y.; Zhao, X.-M.; Kim, E.; Whitesides, G. M. *Chem. Mater.* **1995**, *7*, 2332.

(36) Xia, Y.; Kim, E.; Whitesides, G. M. *J. Electrochem. Soc.* **1996**, *143*, 1070.